ELSEVIER

Journal of Molecular Liquids 129 (2006) 101 – 107

journal of MOLECULAR LIQUIDS

www.elsevier.com/locate/molliq

Relation between hydrogen bonding and intramolecular motions in liquid and supercritical methanol

Jean-Michel Andanson *, Philippe A. Bopp, Jean-Christophe Soetens

Université Bordeaux 1 Laboratoire de Physico-Chimie Moléculaire (UMR 5803), 351 Cours de la Libération F-33405 Talence CEDEX, France

Available online 20 September 2006

Dedicated to professor Gábor Pálinkás on the occasion of his 65th birthday

Abstract

Molecular dynamics (MD) simulations of liquid and supercritical methanol have been performed using a well known flexible 3-sites model. The analysis of the hydrogen bond network has been carried out using first standard geometric criteria on dimers. We then analyzed the effect of hydrogen bonds on single-molecule properties by studying the vibrational and librational motions of a molecule in terms of specific autocorrelation functions and their Fourier transforms. This approach led to an alternative definition of the hydrogen bond, based on molecular properties that can be compared directly with results from molecular spectroscopies (infrared and Raman). It is found that geometric and "spectroscopic" criteria lead to consistent average results over a wide range of thermodynamics conditions while individual molecular results can be different.

Keywords: Molecular dynamics; Autocorrelation functions; Spectroscopies; Hydrogen bonding

1. Introduction

Simulation studies of liquid alcohols, in particular of methanol (MeOH), are plentiful (see e.g. [1–13]) and studies of liquid mixtures containing MeOH are also available [14–24] while simulation studies of supercritical MeOH are scarcer [25]. Here we endeavor to study MeOH over a wide range of thermodynamic conditions with a particular focus on supercritical states. More specifically, we intend to study the hydrogen bonding and the resulting hydrogen-bonded aggregates. This study is in part motivated by a parallel investigation of hydrogen bonding in various alcohols by Infrared and Raman spectroscopies [26,27].

Even though quite sophisticated simulation techniques are available and have been tested on mixtures containing MeOH [15,16], the number of simulations needed to explore different thermodynamic conditions and the lengths of the runs required to accumulate a sufficient number of events — in particular in supercritical states, where fluctuations can be expected to be large — precludes any such approach here. On the other hand, classical Molecular Dynamics (MD) simulations have been shown to be well suited, at least in the liquid state, to obtain the information that we seek. Many interaction models have been developed for MeOH [2–5,7,8,11]. We have selected, for reasons discussed below, the flexible three-site model developed by Pálinkás et al. [2] and known under the acronym "PHH-model".

The structure of the paper is as follows: First, the choice of interaction model will be justified and simulation details will be reviewed. We shall then investigate the hydrogen bonding with the two different approaches alluded to above: One based on structural considerations and a second one based on the perturbations of the molecular motions. These two approaches will be compared with each other and with experimental findings. Drawing from this comparison confidence in the modeling results, a more detailed analysis of the simulations will be presented.

2. Choice of model and details of simulation

The basic requirements to our simulation model can be briefly summarized as follows:

— Since many, and long, runs will be needed, the model should be simple and computationally efficient. This favors a three-site model [2] (hydrogen/oxygen/methyl-group) over a six-

* Corresponding author. Present address: Department of Chemical Engineering, Bone Building, South Kensington Campus, Imperial College, London SW7 2AZ, UK.

E-mail address: jc.soetens@lpcm.u-bordeaux1.fr (J.-C. Soetens).

0167-7322/$ - see front matter © 2006 Elsevier B.V. All rights reserved.
doi:10.1016/j.molliq.2006.08.019

site model [3–5,11] (carbon and hydrogen atoms of the methyl group treated as separate interaction sites).
— The model should be well tested in as many systems as possible.
— Since the densities of the systems to be studied will vary within a factor of 3 or 4, averaged molecular polarizations, like in effective models, may not do and (some) explicit polarizability is desirable [7,8].
— The model should give access to vibrational frequencies, at least to the one associated mostly with the O–H oscillator. Even though this can in principle be achieved in a perturbation theory approach [28], a flexible model is strongly preferred here.

These requirements are, in our opinion, best fulfilled by the PHH model [2], even though we do recognize that there are also drawbacks. Thus, the exact critical point of this model is not known. Furthermore, while the flexibility of the model does entail some polarizability, it is too small, at least compared to usual molecular polarizabilities. Also, the vibrational frequencies have been adjusted, similar to the BJH-model for water [29], by fitting the intramolecular anharmonicities. This, and the missing modes associated with the methyl group, allows in principle to compute only frequency shifts, not absolute frequencies. Last but not least, the fast O–H motions require a small integration time step.

The all-atom model proposed by McDonald et al. [30] was used for the CCl4 molecule, needed in a few preliminary runs, performed for calibration purposes, see section IV-B. Since they are not critical for our purposes, the MeOH–CCl_4 interactions for these runs were simply derived on the basis of TIPS parameters for methanol [1] and the usual Lennard–Jones combining rules.

Details for the four major simulation runs for pure MeOH are listed in Table 1. The thermodynamic conditions for the supercritical (SC) runs were the ones used in parallel experiments [31]. They are sufficiently far away from the critical point that small uncertainties about it's exact numerical values for the model should not matter. The simulation box contained 452 molecules, leading to box-lengths from 31.4 Å in the liquids to 52.7 Å at the lowest density. As mentioned, a short time-step of 0.2 fs was used because of the fast intramolecular motions (O–H vibrational frequencies beyond 3000 cm^{-1}). Cubic periodic boundary conditions were used and a double cutoff for the

Table 1
Molecular dynamics simulations of pure MeOH, characteristic results obtained for the different thermodynamic conditions

Run	Density	T	$<E_{Pot}>$	Self-diff. coeff.	$g(r)$ Characteristics of first peak					
	(g cm^{-3})	(K)	(kJ/mol)	(10^{-9} m^2 s^{-1})	r_{max}^{OH}	r_{min}^{OH}	$n_{r_{min}^{OH}}$	r_{max}^{OO}	r_{min}^{OO}	$n_{r_{min}^{OO}}$
Liq.	0.778	298	−27.1	4.8	1.91	2.67	0.96	2.84	3.42	1.90
SC1	0.478	523	−12.0	30.9	2.00	2.69	0.46	2.89	3.45	1.00
SC2	0.319	523	−8.6	75.5	2.00	2.69	0.33	2.93	3.50	0.75
SC3	0.164	523	−4.9	140.0	2.00	2.69	0.19	2.92	3.50	0.47

The self-diffusion coefficients have been computed from the velocity autocorrelation functions of the molecular centers of mass. For the radial distribution function $g(r)$, r_{max} is the position of the first maximum, r_{min} is the position of the first minimum, and $n(r_{min})$ is the coordination number obtained by integration of the $g(r)$ function up to this first minimum.

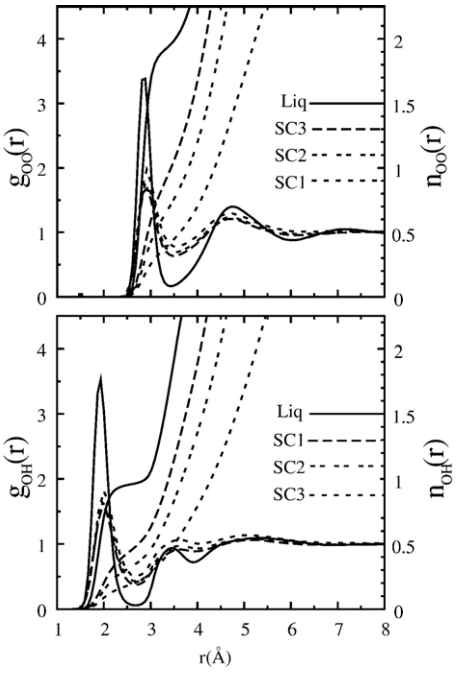

Fig. 1. Oxygen–oxygen (top) and oxygen–hydrogen (bottom) radial distribution functions $g(r)$ and running coordination numbers $n(r)$ for supercritical methanol at 523 K and different densities as well as in the liquid.

interactions was used: 10 Å for the van der Waals interactions and half of the box edge for electrostatic interactions. The simulations were run under NVE-conditions with the MDpol [32] program package. The simulation time was usually 100 ps (500,000 time steps) after equilibration. In smaller and shorter preliminary runs (see Section 4), we have worked with 253 CCl_4 and 2 methanol molecules in a cubic box with the same periodic boundary conditions, cutoffs and time steps as above.

Fig. 1 shows the radial pair distribution functions (rdf) $g_{OO}(r)$ and $g_{OH}(r)$ as well as the running coordination numbers $n_{OO}(r)$ and $n_{OH}(r)$ for the four pure MeOH systems. Characteristic data of the first peak have been collected in Table 1. We shall discuss these functions in more detail below. In the liquid, the average intermolecular potential energy $<E_{pot}>$, partial distribution functions $g(r)$ and the self-diffusion coefficients show the usual kind of agreement with literature values obtained with different [3,25] and the same [2] models. Simulation of supercritical MeOH have been performed by Chalaris and Samios [25] at the same temperature and slightly higher density and our present results show similar tendency for the properties cited above. The aim of the present study being to investigate the hydrogen bonding, the next sections describe in details the two methods used to investigate these properties and the different results obtained.

3. Hydrogen-bond analysis I: geometrical criteria

3.1. Methodology

Analyses of hydrogen bonding in computer simulations generally rest on investigations of local geometries. A first step, at the two particle level, is the examination of the atom–atom partial distribution functions $g_{OH}(r)$ and $g_{OO}(r)$. In water and alcohols, the

Table 2
Fraction f (in %) of molecules having 0, 1, 2, 3 hydrogen bonds, fraction c (in %) of molecules being a member of a cluster with 1 to 6 members, average number of hydrogen-bonds per molecule$<n_{HB}>$, and percentage of free OH obtained from different molecular dynamics simulations with both hydrogen bond definitions (see text)

Run	Geometric definition												Vibrational definition	
	Fraction (in %)				Cluster distribution (%)						$<n_{HB}>$	Free OH %	% free OH	
	f_0	f_1	f_2	f_3	c_1	c_2	c_3	c_4	c_5	c_6		(%)	Q_1	R_2
Liq.	1.5	19.1	68.8	10.6	1.5	1.2	1.3	1.4	1.7	1.6	1.89	5.6	17.0	14.2
SC1	42.2	41.6	15.2	1.0	42.2	23.1	14.1	8.4	5.0	2.9	0.75	61.4	58.2	59.4
SC2	56.4	34.7	8.6	0.3	56.4	22.6	11.0	5.2	2.6	1.2	0.51	74.9	67.7	69.6
SC3	73.3	23.3	3.3	0.1	73.3	18.0	5.8	2.0	0.6	0.2	0.31	85.4	76.7	80.7

relative positions of the first deep minima in these functions indicate a pronounced local structure which has been associated with hydrogen bonding. Going beyond the two particle level, more sophisticated criteria have been devised to make the definitions more stringent or selective. They concern mostly the relative orientations of the two molecules. In these criteria, the values of the positions of the minima in the $g_{OH}(r)$ and $g_{OO}(r)$ functions have often been chosen as upper "cutoff distances" — called here r^C_{OH} and r^C_{OO}, respectively, — above which no bond is considered to exist. We note here, however, that r^C_{OH} and r^C_{OO} will vary with thermodynamic conditions. In terms of angles, a maximum bond-angle ϕ^C(H–O···O) is often used, and a specific way to determine its value has been proposed by Luzar and Chandler [33].

As an aside: an energetic criterion for hydrogen bonding, based on a threshold energy value determined by the positions of the minimum in the pair energy distribution, has also been proposed. Kalinichev and Bass [34] have shown, in the case of water, that under normal conditions both kinds of criteria lead to consistent results. However, in this case, they suggest to use a combination of both under supercritical conditions.

The main advantage of the geometric (and energetic) criteria is their simplicity. Only "standard" informations, available during any simulation (MD and Monte Carlo (MC)), whatever the interaction model used, is required. Each calculation rests on only one configuration (one time-step). Moreover, the geometric criteria allow to distinguish easily the donor or acceptor character of each molecule involved in a hydrogen bonded dimer. Each configuration during a simulation is thus analyzed in detail in order to determine the number of hydrogen bonds, to classify (bin) the molecules according to the number of hydrogen bonds in which they are involved, etc. Averages are simply computed from these individual analyses. Oriented graph representation of the hydrogen bond network can be constructed and studies have been devoted to such topological analyses for both alcohols [35] and water [36–38]. Instead of using individual time steps, such analyses can also be carried out on configurations averaged over various short periods of time in order to filter out fast motions (vibrations, librations).

3.2. H-bond criterion

The values for $n_{r^{min}_{OO}}$ *and* $n_{r^{min}_{OH}}$ (intramolecular O–H peaks omitted), reported in Table 1, are often taken as a first approximation to the number of hydrogen bonds: The average number of hydrogen bonds,$<n_{HB}>$, is then defined either as 2 $n_{r^{min}_{OH}} = <n_{HB}>$ (i.e. two times the number of donor molecules) or simply $n_{r^{min}_{OO}} = <n_{HB}>$.

Since in the present case the positions (not the depths) of the minima do not vary much with thermodynamic conditions (see Table 1), and to be consistent with previous works [6,10,25], we have chosen r^C_{OO}=3.5 Å, r^C_{OH}=2.6 Å and ϕ^C=30° as upper cutoff limits for our geometric definitions. It turn out that the distance criteria are the more stringent ones and that results are only weakly dependent on reasonable variations of ϕ^C. All analyses in the next section are based on this criterion.

3.3. Results

Table 2 lists the fractions f_i of molecules in the system having i= 0, 1, 2, 3 hydrogen bonds. This definition of the fs is similar to the one used by Padró et al. [10] and Chalaris and Samios [25] in their work. The average number of hydrogen bonds per molecule $<n_{HB}>$ and the percentage of O–H oscillators without bonding (called "% free OH") is also listed for later comparison.

In the liquid, each molecule is, on the average, engaged in about 1.9 hydrogen bonds (one donor, one acceptor, say) while in the supercritical regime this values decrease to less than 1.0 and down to 1/3 at the lowest density, even though there is no dramatic evolution in the radial distribution functions.

We have also constructed at each time step a connectivity matrix in order to perform a topological analysis of the hydrogen bond network in terms of clusters (see for comparison e.g.

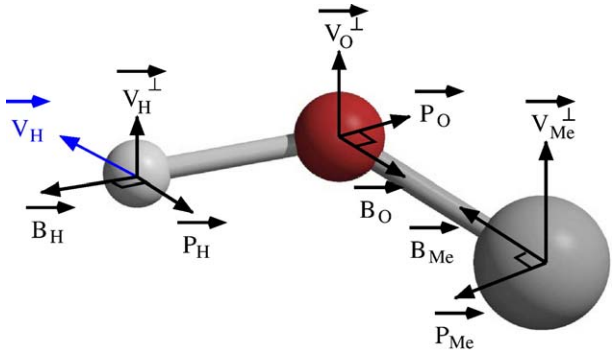

Fig. 2. Decomposition of the atom velocities, in the center of mass system of the molecule, into vectors with magnitudes of: $V^{\perp}$ perpendicular to the molecular plane, B in direction of the bond, and P perpendicular to the bond. The total velocity is indicated for the hydrogen only (V_H).

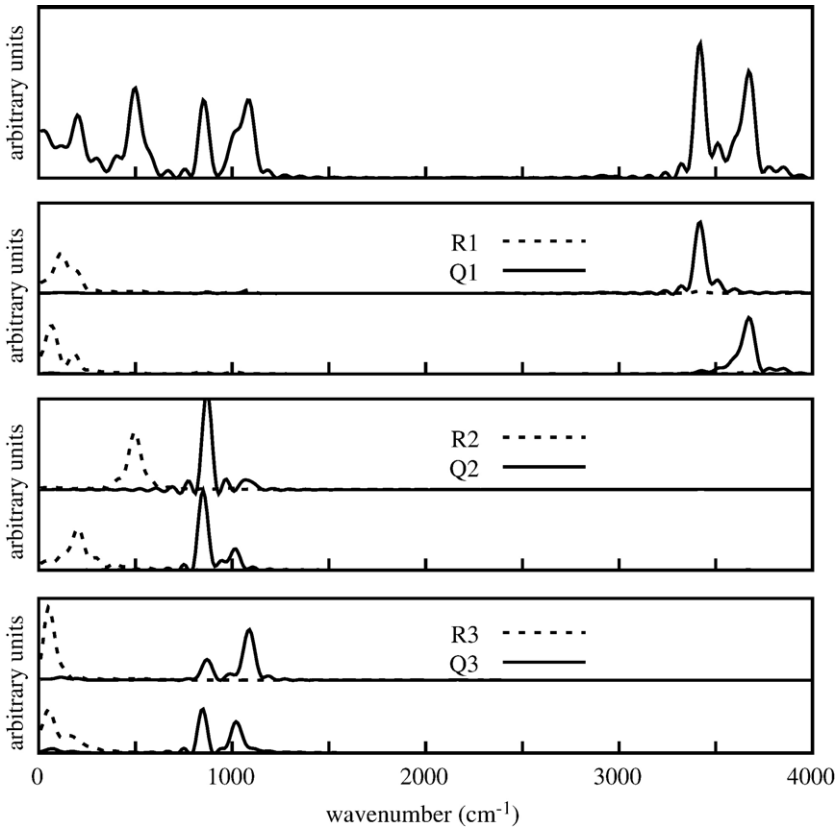

Fig. 3. Spectral densities obtained from a selected window of 10 ps (see text) from an MD simulation of a methanol dimer in 256 rigid CCl_4 molecules. Top: Spectral density from the total velocities of both hydrogen atoms. (Note the non-zero value for $I(\omega=0)$, proportional to the self-diffusion coefficient.) Pairs of panels below: Fourier transforms of the autocorrelation functions of the Qs and Rs defined in the text: Upper panel of each pair: Molecule identified as donor; lower panel: acceptor.

[35,39]). The percentages of molecules involved in clusters of sizes up to the hexamer, which have been observed to be the more significant structures in our systems, are also reported in the Table 2. All cluster sizes studied here are equally represented in the liquid, the vast majority of molecules being incorporated in much larger clusters. In the supercritical fluids, the largest fraction of molecules are monomers, and the population of higher aggregates decreases roughly exponentially. The fraction of monomers increases strongly with decreasing density. Overall, at this temperature, the fraction of molecules included in clusters of size less than 5 is 0, 93, 0.98, and 0.997 for the three densities, respectively. In liquid the corresponding fraction is 0.07.

The percentage of free hydroxyl group can be computed using both hydrogen bonds criteria, see below. We note first that this number is not immediately computable from the *f*-values because of the varied topology of the aggregates: Linear and bifurcated chains, rings, and combinations thereof.

4. Hydrogen-bond analysis II: intramolecular motions

4.1. Methodology

Classical infrared or Raman hydrogen-bond spectroscopy rests on the observation of the high frequency oscillators involving mostly heavy-atom-H motions, perturbed by the bonding. The most striking observations are down-shifts (redshifts) of this frequency compared to the corresponding frequency of the isolated molecule. Already a long time ago these have been empirically related to various features of the H-bond [40], e.g. its "strength". In keeping with this approach, we propose here, as it has already been done previously [14], to observe the intramolecular motions of our model-MeOH and relate their frequency shifts to the hydrogen bonding.

At any time step during an MD simulation each methanol molecule in the system is characterized by the positions and velocities of hydrogen, oxygen and the methyl group. Using appropriate combinations and projections of the velocities [14], it is possible to extract normal mode like combinations. First, the center of mass velocity is subtracted from the sites velocities in order to remove the molecular translations. Then these 'relative' atomic velocities are decomposed into their components perpendicular and parallel with respect to the instantaneous plane of the molecule. Finally, the in-plane components are decomposed into the directions parallel and perpendicular to the bond. Nine components are obtained, as shown in Fig. 2. The following combinations lead to six quantities ($Q_{1,2,3}$ and $R_{1,2,3}$) which approximate vibrational and rotational (librational) movements [14]:

$Q_1=B_H$	O–H stretching
$Q_2=B_{Me}+B_O$	O–Me stretching
$Q_3=P_H+P_{Me}$	H–O–Me bending
$R_1=P_O+P_{Me}$	Rotation in plane
$R_2=V_H^{\perp}$	Rotation of H roughly around the O–Me bond
$R_3=V_O^{\perp}-V_{Me}^{\perp}$	Rotation roughly around an axis perpendicular to the O–Me bond

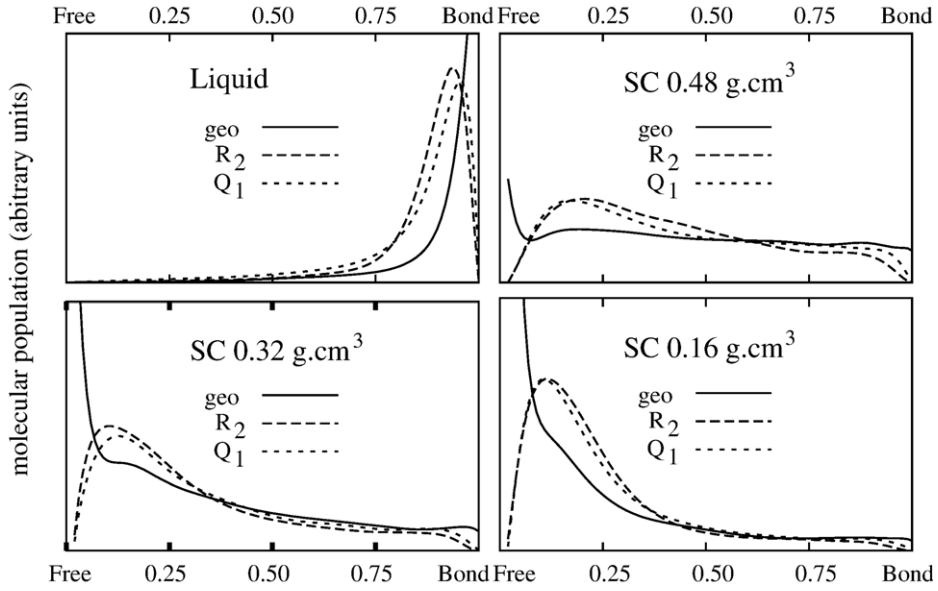

Fig. 4. Number of methanol molecules being hydrogen bonded according to the geometrical (solid lines) and the spectroscopic definition (long dashes: R_2, short dashes: Q_1) during a (not necessarily continuous) fraction of a 2 ps time window (see text).

The autocorrelation functions $C_{aa}(t)$, $a=Q_i$ or R_i, of these quantities and their Fourier transforms, the spectral densities of motion $I_{aa}(\omega)$, scan be computed according to the following equations

$$C_{aa}(t) = <a(t) \,.\, a(0)> \tag{4.1}$$

$$I_{aa}(\omega) = \int_0^\infty C_{aa}(t) \,.\, \cos(\omega t) \,.\, \mathrm{d}t \tag{4.2}$$

We note that the peak positions in $I_{aa}(\omega)$, but not the peak intensities, can by identified with the peaks observed in vibrational spectroscope.

4.2. Calibration: the methanol dimer in CCl_4

In order to probe the feasibility of a hydrogen-bond definition based on intramolecular motions for our purposes, we have first studied a simple system: a single methanol dimer embedded in CCl_4. The spectral densities displayed in Fig. 3 were obtained from a 10 ps window in this simulation where, by visual inspection, the same hydrogen bond between the two molecules persists. Beyond this window, events are observed where, through a collective motion of the two molecules, the molecule donating the bond becomes the acceptor and vice versa. This is an interesting finding, it will, however, be left to further, more thorough investigations. Fig. 3 shows the spectral density obtained from the velocities of the two hydrogen atoms (top) and below, separately for the two molecules, the densities obtained from the autocorrelations of the Qs and Rs defined above. While all information is inherently present in the spectral density of the hydrogen velocities, it can be only disentangled by looking at the combinations of projections Q and R. The figure shows that the modes most strongly affected by the bonding are Q_1 and R_2, we shall therefor focus on these here. We note the following features

- The frequency of the peak maximum for the Q_1 mode shows a redshift of about 200 cm^{-1} between acceptor molecules (free OH) and donor molecule (bonded OH).
- The frequency of the peak maximum for the R_2 mode shows a blue-shift of about 250 cm^{-1} between acceptor molecules and donor molecule.

The analysis of the spectral densities showing a clear correlation between the bonding situation (hydrogen bond donor) and the frequencies of the modes Q_1 and R_2, we propose (after some tests concerning the limits of integration) to determine the percentage of free OH in pure liquid methanol according to the following procedure

- The individual Q_1 and R_2 spectral densities of each molecule are determined from autocorrelation functions of 500 fs length. Each correlation function is averaged over a time window of 2 ps. In order to avoid spurious oscillations in the Fourier transforms, it is damped between 450 fs and 500 fs by an exponential function before transformation.
- As the hydrogen bond lifetime is of the order of picoseconds, an individual spectral density can display both donor and acceptor peaks. The percentage of 'free OH' in the system is then computed as an average of individual integrals during the simulation according to the following relation

$$\textit{For } Q_1: \quad \%\text{free OH} = \left\langle \frac{\int_{3100\ \mathrm{cm}^{-1}}^{3900\ \mathrm{cm}^{-1}} I_{Q_1}(\bar{\nu})\ \mathrm{d}\bar{\nu}}{\int_{3500\ \mathrm{cm}^{-1}}^{3900\ \mathrm{cm}^{-1}} I_{Q_1}(\bar{\nu})\ \mathrm{d}\bar{\nu}} \right\rangle \text{ molecules time windows} \tag{4.3}$$

$$\text{For } R_2: \quad \%\text{free OH} = \left\langle \frac{\int_{0\ \mathrm{cm^{-1}}}^{380\ \mathrm{cm^{-1}}} I_{R_2}(\bar{\nu})\ \mathrm{d}\bar{\nu}}{\int_{0\ \mathrm{cm^{-1}}}^{800\ \mathrm{cm^{-1}}} I_{R_2}(\bar{\nu})\ \mathrm{d}\bar{\nu}} \right\rangle \text{ molecules time windows} \tag{4.4}$$

where $I_{Q_1}(\nu)$ and $I_{R_2}(\nu)$ are the spectral densities of the quantities of Q_1 and R_2 for a single molecule, respectively. For the sake of simplicity we shall call this the "spectroscopic" definitions.

4.3. Results

Results obtained from this analysis are also collected in Table 2 (last columns). Of course, since this definition rests only on one molecule, its neighbors are not known without further assumptions, and the properties reported for the geometric definition (e.g. the topological analyses) cannot be obtained. We note first the good agreement between the percentages of "free OH" obtained from Q_1 and R_2. In the supercritical cases, the agreement is also good with the value obtained with the geometric criterion. It is less satisfactory for the liquid. In this case the percentage of free OH is very low and the numerical integration (Eqs. (4.3) and (4.4)) can lead to these discrepancies. Furthermore, the correlation times of the oscillators being shorter here (see e.g. Ref. [14]), the bands are broadened.

5. Comparison of both methods

In order to compare in more detail the results obtained with the two classes of hydrogen bond definitions, Fig. 4 shows the histogram of molecules being bonded during a certain (not necessarily contiguous) fraction of a time window of 2 ps. For the geometric definition the abscissa corresponds to the ratio of "bonded" to total cases found for individual molecules. For the spectroscopic definition, it is the histogram of the ratios inside the <> — brackets in Eqs. (4.3) and (4.4).

In the liquid, in keeping with the percentages of "free OH" given in Table 2, the positions of the maxima of the distributions are around 1:0, which corresponds to a large amount of hydrogen bonded molecules. However, the dashed curves associated with the spectroscopic definition present a real maxima while the solid curve obtained using the geometric definition increases continuously. This feature indicates that in the latter case, most of the molecules are hydrogen bonded continously over more than 2 ps, while during the same period of time the spectral density can display frequencies associated with both "free" and "bonded" OH. This may be related to the finite relaxation time of the oscillators. In the supercritical fluids, the maxima shift to the left-hand side of the distributions. The height of the maxima increases with the decreasing density. The observation made above for the upper end of the distribution applies here at the lower end.

Fig. 5 shows a 2-dimensional representation correlating the average frequency of the Q_1 mode with the average O–O and O–H nearest neighbor distances for a central molecule, the averages being taken over the usual 2 ps time windows. The dashed lines indicate the limiting values for the two H-bonding criteria. Similar graphs can be generated with the R_1 frequencies, however, as can be expected from Fig. 4, no new independent information is gained. In these graphs, intensity in the lower left and upper right quadrants stems from molecules fulfilling (lower left), or not (upper right), simultaneously the spectroscopic and one of the geometric criteria. It is seen that in the liquid the main intensities are indeed in the lower left quadrants, indicating a high degree of hydrogen bonding. However, we note some intensity in the lower right quadrant, i.e. molecules geometrically hydrogen bonded but displaying frequencies higher than the integration limit (Eqs. (4.3) and (4.4)). This was already noted in the discussion of Fig. 4 and ascribed to the finite relaxation times of the oscillators.

In the supercritical cases, increasing intensity is observed, as expected, in the upper right quadrants, the non-bonded molecules. However, there is also a marked increase in the lower right and, less so, in the upper left quadrants. In the correlations with the O–O distances, a large fraction of the intensity in the lower left quadrants, in particular the peak seen there, stems from molecules accepting H-bonds from neighbors in dimers (i.e. molecules with

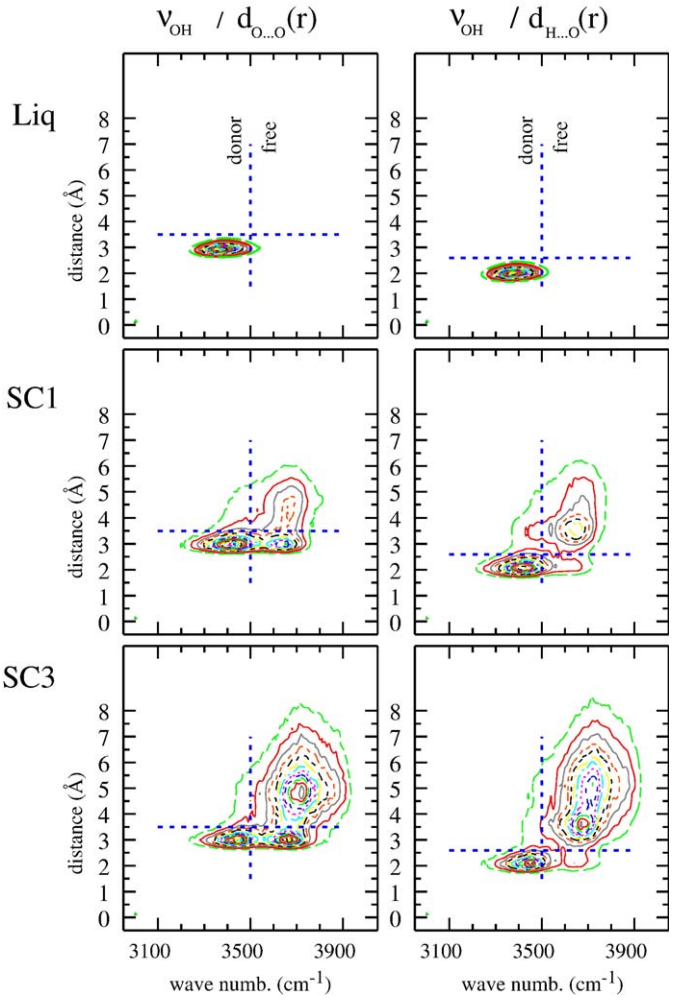

Fig. 5. Correlation diagrams between the average O–O (left) and O–H (right) distances with the nearest neighbor and the position of the peak maximum of the Fourier transform of I_{Q_1} in a 2 ps time window. The dotted lines are just guides to the eyes and indicate the geometrical hydrogen bonding criteria (see Section 3).

non-bonded O–H groups). The more diffuse intensity in these regions is again due to the slow (slower in the SC systems than in the liquid) relaxation of the oscillators moving into (and in the upper left quadrant out of) bonds.

The most striking feature, however, is the wide distribution of 'nearest neighbor'-distances and associated frequencies revealed in the upper right quadrants. This reflects the large fluctuations in the SC systems. Due to these fluctuations, the neighborhood experienced by a molecule becomes increasingly heterogeneous and changes rapidly. It is surprising that even under these circumstances the vast majority of molecules can be unambiguously classified according to the two criteria as 'bonded' or 'non-bonded', the O–H distance being a better choice here than the O–O distance. Thus, particularly in the SC cases, discrepancies between geometric and vibrational criteria are seen when individual molecules are considered. On the average over all molecules, however, good agreement is found, as reported above in Table 2.

6. Summary and conclusion

The notion of 'hydrogen-bond' is not inherent to most models used in molecular simulations. The existence of such bonds must thus be established *post factum* by examining the generated configurations according to suitable criteria. We have compared here two such criteria, a 'geometric' one and a 'spectroscopic' one, akin to the one used in vibrational spectroscopies, for methanol in the liquid and in several supercritical states. The overall result is that a quite satisfactory agreement is found between both criteria. When looking at individual molecules in the supercritical states, however, the agreement deteriorates, while it remains good when averages over the whole system are considered. With this caveat in mind, comparisons between experimental (e.g. IR) spectra and simulation results can be made in the supercritical phases in the same way as they have been made in liquids.

Acknowledgments

Computer time for this study was in parts provided on its workstations by UFR de Chimie of Université Bordeaux 1 and by Pôle M3PEC of this University on its IBM p690. Other runs were carried out on local Linux boxes. JMA received a research bursary from the French Ministry of Education and Research. Many thanks are also due to Marcel Besnard, Thierry Tassaing, and Yann Danten for their fruitful discussions.

References

[1] W.L. Jorgensen, M. Ibrahim, J. Am. Chem. Soc. 104 (1982) 373.
[2] G. Pálinkás, E. Hawlicka, K. Heinzinger, J. Phys. Chem. 91 (1987) 4334.
[3] W.L. Jorgensen, J. Phys. Chem. 90 (1986) 1276.
[4] E. Hawlicka, G. Pálinkás, K. Heinzinger, Chem. Phys. Lett. 154 (1989) 255.
[5] E.H.S. Anwander, M.M. Probst, B.M. Rode, Chem. Phys. 116 (1992) 341.
[6] J. Martı, J. Padró, E. Guárdia, J. Mol. Liq. 64 (1995) 1.
[7] J.W. Caldwell, P.A. Kollman, J. Phys. Chem. 99 (1995) 6208.
[8] J. Gao, D. Habibollazadeh, L. Shao, J. Phys. Chem. 99 (1995) 16460.
[9] S.L. Wallen, B.J. Palmer, B.C. Garrett, C.R., J. Phys. Chem. 100 (1996) 3959.
[10] J. Padró, L. Saiz, E. Guárdia, J. Mol. Struct. 416 (1997) 243.
[11] L. Bianchi, A.K. Adya, C.J. Wormald, J. Phys., Condens. Matter 11 (1999) 9151.
[12] I. Bakó, P. Jedlovszky, G. Pálinkás, Chem. Phys. Lett. 87 (2000) 243.
[13] M. Pagliai, G. Cardini, R. Righini, V. Schettino, J. Chem. Phys. 119 (2003) 6655.
[14] G. Pálinkás, I. Bakó, K. Heinzinger, P. Bopp, Mol. Phys. 73 (1991) 897.
[15] A. Staib, D. Borgis, Chem. Phys. Lett. 271 (1997) 232.
[16] A. Staib, J. Chem. Phys. 108 (1998) 4554.
[17] R. Veldhuizen, S.W. de Leeuw, J. Chem. Phys. 105 (1996) 2828.
[18] M. Ferrario, M. Haughney, I.R. McDonald, M.L. Klein, J. Chem. Phys. 93 (1990) 5156.
[19] D. Marx, K. Heinzinger, G. Pálinkás, I. Bakó, Z. Naturforsch. 47a (1991) 887.
[20] Y. Tamura, E. Spohr, K. Heinzinger, G. Pálinkás, I. Bakó, Ber. Bunsen. Phys. Chem. 96 (1992) 147.
[21] E. Hawlicka, D. Swiatla-Wojcik, Chem. Phys. 195 (1995) 221.
[22] E. Hawlicka, D. Swiatla-Wojcik, Chem. Phys. 218 (1997) 49.
[23] E. Hawlicka, D. Swiatla-Wojcik, J. Phys. Chem., A 106 (2002) 1336.
[24] E. Hawlicka, D. Swiatla-Wojcik, J. Chem. Phys. 119 (2003) 2206.
[25] M. Chalaris, J. Samios, J. Phys. Chem., B 103 (1999) 1161.
[26] P. Lalanne, J.M. Andanson, J.C. Soetens, T. Tassaing, Y. Danten, M. Besnard, J. Phys. Chem., A 108 (2004) 3902.
[27] J.M. Andanson, J.C. Soetens, T. Tassaing, M. Besnard, J. Chem. Phys. 122 (2005) 174512.
[28] G. Heinje, W.A.P. Luck, P.A. Bopp, Chem. Phys. Lett. 152 (1998) 358.
[29] P. Bopp, J. Jancsó, K. Heinzinger, Chem. Phys. Lett. 98 (1983) 129.
[30] I.R. McDonald, D.G. Bounds, M.L. Klein, Mol. Phys. 45 (1982) 521.
[31] M. Hoffman, M. Conradi, J. Phys. Chem., B 102 (1998) 263.
[32] J.C. Soetens PhD Thesis, Université Henri Poincaré - Nancy I, 1996.
[33] A. Luzar, D. Chandler, J. Chem. Phys. 98 (1990) 8160.
[34] A. Kalinichev, J. Bass, J. Phys. Chem., A 101 (1997) 9720.
[35] I. Shilov, B. Rode, V. Durov, Chem. Phys. 241 (1999) 75.
[36] A. Geiger, F. Stillinger, A. Rahman, J. Chem. Phys. 70 (1979) 4185.
[37] R. Blumberg, H. Stanley, A. Geiger, P. Mausbach, J. Chem. Phys. 80 (1984) 5230.
[38] D. Bergman, Chem. Phys. 253 (2000) 267.
[39] V.V. Zakharov, E.N. Brodskaya, A. Laaksonen, J. Chem. Phys. 109 (1998) 9487.
[40] R.M. Badger, S.H. Bauer, J. Chem. Phys. 5 (1937) 2839.